



High Catalytic Activity of Heteropolynuclear Cyanide Complexes Containing Cobalt and Platinum Ions: Visible-Light Driven Water Oxidation**

Yusuke Yamada,* Kohei Oyama, Rachel Gates, and Shunichi Fukuzumi*

Abstract: A near-stoichiometric amount of O_2 was evolved as observed in the visible-light irradiation of an aqueous buffer (pH 8) containing $[Ru^{II}(2,2'-bipyridine)_3]$ as a photosensitizer, $Na_2S_2O_8$ as a sacrificial electron acceptor, and a heteropolynuclear cyanide complex as a water-oxidation catalyst. The heteropolynuclear cyanide complexes exhibited higher catalytic activity than a polynuclear cyanide complex containing only Co^{III} or Pt^{IV} ions as C-bound metal ions. The origin of the synergistic effect between Co and Pt ions is discussed in relation to electronic and local atomic structures of the complexes.

The increasing demand by human beings for energy encourages researchers to study artificial photosynthesis, in which high-energy compounds are produced from water as an electron donor, by utilizing solar energy.^[1–3] A bottleneck to realizing artificial photosynthesis is the low activity of water oxidation catalysts.^[4,5] A wide variety of homogeneous and heterogeneous catalysts have been examined for water oxidation.^[6,7] Metal complexes, often used as homogeneous catalysts, are advantageous for designing the active species, however, their low stability causes a problem in identifying an active species.^[8] Metal oxides have also been extensively studied in heterogeneous systems as robust water-oxidation catalysts (WOCs), although their catalytically active species remain equivocal in multiple component systems.^[9] Recently, coordination polymers emerged as potential candidates, possessing both designable structures at the atomic level and robustness under harsh reaction conditions.^[10]

Heteropolynuclear cyanide complexes are the simplest class of coordination polymers. In general, heteropolynuclear cyanide complexes have a cubic structure as far as the contained metal ions allow octahedral coordination.^[11] Both C and N atoms of cyanide interact with metal ions, however, a C atom tends to coordinate to a metal ion more strongly. When the number of N-bound metal ions is larger than that of C-bound metal ions, the N-bound metal ions need external ligands, such as an aqua ligand, to fulfill the octahedral coordination. In such a case, the aqua ligands can be liberated from the N-bound metal ions in a reaction solution to provide substrate-binding sites.^[12] The number of external ligands can be controlled by considering charge compensation in a heteropolynuclear complex.^[12] Additionally, the character of the N-bound metal ion can be influenced by the C-bound metal ion through $\pi\pi$ - $d\pi$ interactions between a cyanide ligand and the metal ions.^[13] Thus, heteropolynuclear cyanide complexes can be easily modified as heterogeneous catalysts suitable for water oxidation.

We report herein visible-light driven water oxidation catalyzed by heteropolynuclear cyanide complexes containing both cobalt and platinum ions where Co^{III} and Pt^{IV} ions are employed as C-bound metal ions and Co^{II} ions as N-bound metal ions. They are superior to polynuclear cyanide complexes which contain only cobalt or platinum ions as C-bound metal ions. The higher oxidation state of Pt^{IV} than that of Co^{III} can be expected to enhance the oxidation ability of Co^{II} ions. When heteropolynuclear cyanide complexes contain coordinatively unsaturated Pt^{II} ions instead of coordinatively saturated Pt^{IV} ions, the number of defect sites increases within the framework, thus resulting in an increase in the number of active sites accessible by a substrate molecule. Both electronic and structural effects are examined for a series of cyanide complexes by changing the content of the platinum ions.

The catalysis of the heteropolynuclear cyanide complexes for visible-light driven water oxidation was examined in a reaction solution containing $[Ru(bpy)_3]^{2+}$; $bpy = 2,2'$ -bipyridine) and $S_2O_8^{2-}$ as a photosensitizer and a sacrificial electron acceptor, respectively. The overall catalytic cycle is shown in Scheme 1, where photoexcited $[Ru(bpy)_3]^{2+}$ initiates the reaction by reducing $Na_2S_2O_8$, and $[Ru(bpy)_3]^{3+}$, thus formed, oxidizes the heteropolynuclear cyanide complex which then oxidizes water for O_2 evolution.

A series of the heteropolynuclear cyanide complexes containing Pt^{IV} ions, $[Co^{II}(H_2O)_m]_n[(Co^{III}_{1-x}Pt^{IV}_x)(CN)_6]$, were prepared by mixing an aqueous solution containing both $K_3[Co^{III}(CN)_6]$ and $K_2[Pt^{IV}(CN)_6]$ with various Co^{III}/Pt^{IV} ratios ranging from 1:0 to 0:1, and an aqueous solution

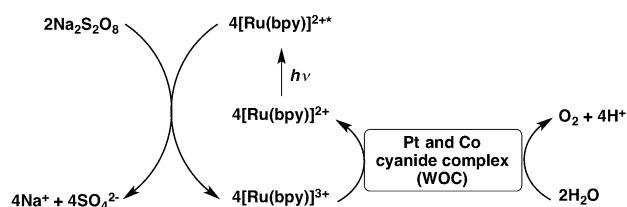
[*] Prof. Dr. Y. Yamada, K. Oyama, Prof. Dr. S. Fukuzumi
Department of Material and Life Science
Graduate School of Engineering, Osaka University
2-1 Yamada-oka, Suita, Osaka 565-0871 (Japan)
E-mail: yamada@chem.eng.osaka-u.ac.jp
fukuzumi@chem.eng.osaka-u.ac.jp
Homepage: <http://www-etchem.mls.eng.osaka-u.ac.jp/>

Prof. Dr. S. Fukuzumi
Department of Bioinspired Science, Ewha Womans University
Seoul 120-750 (Korea)

R. Gates
California Institute of Technology
1200 East California Boulevard, Pasadena, CA 91125 (USA)

[**] This work was supported by an ALCA project from JST (to S.F.) and Grants-in-Aid (Nos. 24350069 and 25600025 to Y.Y.) from the Ministry of Education, Culture, Sports, Science and Technology (Japan).

Supporting information for this article is available on the WWW under <http://dx.doi.org/10.1002/anie.201501116>.



Scheme 1. Overall catalytic cycle of visible-light driven water oxidation.

containing an excess amount of $\text{Co}(\text{NO}_3)_2$. The formed crystalline powder was collected by filtration. The cobalt and platinum ion content of each powder were determined by X-ray fluorescence measurements. The number of Co^{II} ions in a unit cell decreases with an increase in the number of Pt^{IV} ions in a unit cell ($n = 1.5 - 0.5x$). Also, the number of water molecules coordinating to Co^{II} ions decreases from two to zero with an increase in the content of the Pt^{IV} ions ($m = 3(1-x)/n$; see note on page S2 in the Supporting Information). Peaks for the K^+ ions were not observed in any sample, thus indicating that the content of the K^+ ions was lower than 0.12%. Incorporation of Co^{II} ions into the framework was also confirmed by the higher wavenumber of the CN stretching bands [$\nu(\text{CN})$] in the IR spectra (see Figure S1). Powder X-ray diffraction patterns for the heteropolynuclear cyanide complexes with the Pt^{IV} ion content ranging from 0 to 1 are shown in Figure 1a and were assigned as a cubic

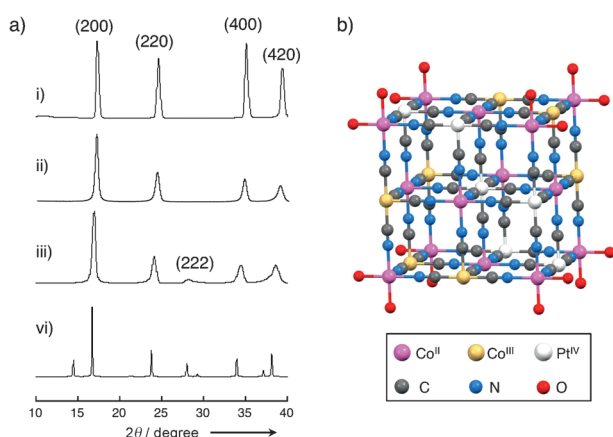


Figure 1. a) Powder X-ray diffraction patterns of a series of heteropolynuclear cyanide complexes, $[\text{Co}^{\text{II}}(\text{H}_2\text{O})_m]_n[\text{Co}^{\text{III}}_{1-x}\text{Pt}^{\text{IV}}_x(\text{CN})_6]_n$. i) $x = 0$, ii) $x = 0.15$, iii) $x = 0.43$, and iv) $x = 1$. b) A schematic drawing of $[\text{Co}^{\text{II}}(\text{H}_2\text{O})_m]_n[\text{Co}^{\text{III}}_{1-x}\text{Pt}^{\text{IV}}_x(\text{CN})_6]_n$. Hydrogen atoms of water molecules are omitted.

structure (Figure 1b), which is often called a Prussian blue analogue structure. The gradual decrease of the diffraction peaks in the 2θ angle in accordance with the increase in the Pt^{IV} ion content and reflects the expansion of a unit cell resulting from the larger ionic radii of a Pt^{IV} ion (0.77 Å) relative to that of a Co^{III} ion (0.69 Å).^[14] Microporous structures of the series of complexes were also evidenced by the Brunauer–Emmett–Teller (BET) surface areas which were higher than $400 \text{ m}^2 \text{ g}^{-1}$ (see Figure S2).

Replacement of Co^{III} ions in $[\text{Co}^{\text{II}}(\text{H}_2\text{O})_2]_{1.5}[\text{Co}^{\text{III}}(\text{CN})_6]$ by Pt^{IV} ions enhances the oxidation ability of the Co^{II} ions. The oxidation potential of the Co^{II} ions in $[\text{Co}^{\text{II}}(\text{H}_2\text{O})_m]_n[\text{Co}^{\text{III}}_{1-x}\text{Pt}^{\text{IV}}_x(\text{CN})_6]_n$ was examined by differential pulse voltammetry (DPV) in an acetonitrile suspension. The peak for oxidation of Co^{II} to Co^{III} in $[\text{Co}^{\text{II}}(\text{H}_2\text{O})_2]_{1.5}[\text{Co}^{\text{III}}(\text{CN})_6]$ (0.67 V vs. Ag/Ag^+) was observed in an anodic sweep. The oxidation peak was gradually shifted in the positive direction to 0.94 V by increasing the Pt^{IV} ion content to 1.0 (Figure 2). The positive shift upon an increase in the

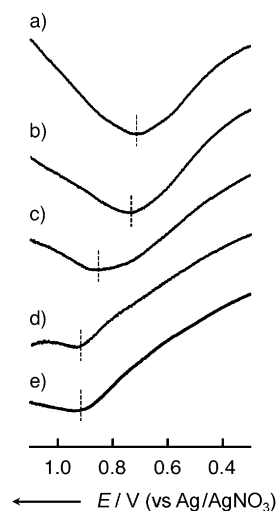


Figure 2. Differential pulse voltammetry of a series of heteropolynuclear cyanide complexes, $[\text{Co}^{\text{II}}(\text{H}_2\text{O})_m]_n[\text{Co}^{\text{III}}_{1-x}\text{Pt}^{\text{IV}}_x(\text{CN})_6]_n$. a) $x = 0$, b) $x = 0.15$, c) $x = 0.43$, d) $x = 0.69$, and e) $x = 1$. The measurements were performed in an acetonitrile (2.0 mL) suspension of $[\text{Co}^{\text{II}}(\text{H}_2\text{O})_m]_n[\text{Co}^{\text{III}}_{1-x}\text{Pt}^{\text{IV}}_x(\text{CN})_6]_n$ (10 μmol) using a glassy carbon electrode, a Pt wire, and an Ag/AgNO_3 electrode as the working electrode, counter electrode, and reference electrode, respectively.

Pt^{IV} ion content is evidence of the electronic interaction between Pt^{IV} and Co^{II} ions. The electronic interaction between the Co^{II} and Pt^{IV} ions also depends on the Pt^{IV} ion content, as evidenced by the shift of the absorption maxima, derived from the metal-to-metal charge transfer band, appearing in the near-IR region (see Figure S3). The absorption band appeared at around 1165 nm for $[\text{Co}^{\text{II}}(\text{H}_2\text{O})_2]_{1.5}[\text{Co}^{\text{III}}(\text{CN})_6]$ ($x = 0$) and was gradually shifted to 1126 nm as the Pt^{IV} ion content in $[\text{Co}^{\text{II}}(\text{H}_2\text{O})_{1.33}]_{1.29}[\text{Co}^{\text{III}}_{0.57}\text{Pt}^{\text{IV}}_{0.43}(\text{CN})_6]$ ($x = 0.43$) was increased. The near-IR bands were assigned to metal-to-metal charge transfer from e_g orbitals of a Co^{II} ion (high spin) to the e_g orbitals of a Co^{III} or a Pt^{IV} ion (low spin).^[15] The positive shift of the oxidation potential of the Co^{II} ion observed in DPV suggests the energy level of the e_g orbital of the Co^{II} ion decreases.

Photocatalytic water oxidation was performed by photoirradiation ($\lambda > 420 \text{ nm}$) of a phosphate buffer (2.0 mL, 50 mM, pH 8.0) containing $[\text{Ru}(\text{bpy})_3]^{2+}$ (1.0 mM), $\text{Na}_2\text{S}_2\text{O}_8$ (5.0 mM), and $[\text{Co}^{\text{II}}(\text{H}_2\text{O})_m]_n[\text{Co}^{\text{III}}_{1-x}\text{Pt}^{\text{IV}}_x(\text{CN})_6]_n$ (80 μg). Time courses of O_2 evolution are indicated in Figure 3a. It was confirmed that there was no O_2 evolution under dark conditions. An insignificant amount of O_2 evolution was observed for the reaction solution containing $\text{Co}^{\text{II}}[\text{Pt}^{\text{IV}}(\text{CN})_6]$.

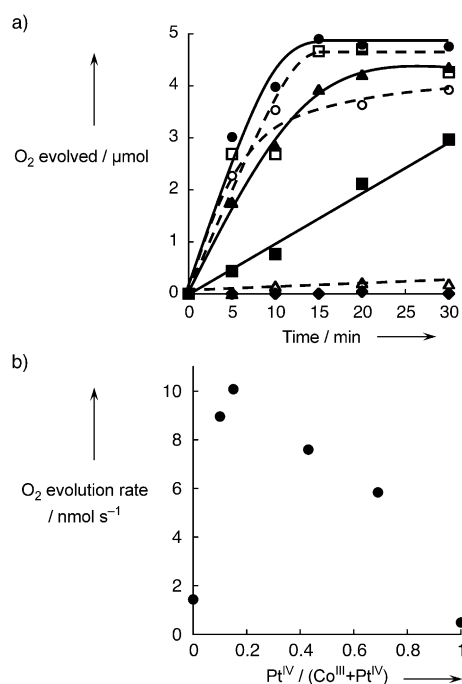


Figure 3. a) Time courses of O₂ evolution by visible-light irradiation ($\lambda > 420$ nm) of a phosphate buffer (2.0 mL, 50 mM, pH 8.0) containing [Ru(bpy)₃]²⁺ (1.0 mM), Na₂S₂O₈ (5.0 mM), and a heteropolynuclear cyanide complex, [Co^{II}(H₂O)_m]_n[(Co^{III}_{1-x}Pt^{IV}_x)(CN)₆] (80 μg). $x = 0$ (closed square); 0.10 (open square); 0.15 (closed circle); 0.43 (open circle); 0.69 (closed triangle) and 1 (open triangle). Time course of O₂ evolution under dark conditions using the complex with $x = 0.15$ (open diamond). b) Initial O₂ evolution rates (< 5 min) at different Pt^{IV} ion contents in [Co^{II}(H₂O)_m]_n[(Co^{III}_{1-x}Pt^{IV}_x)(CN)₆].

In contrast, a significant amount of O₂ evolution was observed for the reaction solution containing [Co^{II}(H₂O)₂]_{1.5}-[Co^{III}(CN)₆], where the O₂ yield (based on the amount of Na₂S₂O₈) reached about 60% after photoradiation for 30 minutes. The O₂ yields were further increased to more than 80% by employing [Co^{II}(H₂O)_m]_n[(Co^{III}_{1-x}Pt^{IV}_x)(CN)₆] ($x = 0.15, 0.43$ and 0.69) as WOCs. In particular, a nearly stoichiometric amount of O₂ (> 98%) was obtained for the reaction system containing [Co^{II}(H₂O)_{1.79}]_{1.42}[(Co^{III}_{0.85}Pt^{IV}_{0.15})(CN)₆] ($x = 0.15$). The initial O₂ evolution rates (< 5 min) were plotted against the Pt^{IV} ion content in [Co^{II}(H₂O)_m]_n[(Co^{III}_{1-x}Pt^{IV}_x)(CN)₆] (Figure 3b). The fastest O₂ evolution was observed for [Co^{II}(H₂O)_{1.79}]_{1.42}[(Co^{III}_{0.85}Pt^{IV}_{0.15})(CN)₆] where the initial O₂ evolution rate exceeded 10 nmol s⁻¹, and is comparable to that reported for the reaction system using IrO₂ nanoparticles, which are known as one of the most active heterogeneous catalysts for the photocatalytic water oxidation at pH 5.^[16]

The Co^{III} and Pt^{IV} ions are coordinatively saturated, thus, N-bound Co^{II} ions can act as active sites by liberating coordinating H₂O molecules. The number of H₂O molecules decreases in proportion to the Pt^{IV} ion content because of charge compensation. In contrast, the oxidation ability of the Co^{II} ions is more enhanced in the presence of a higher content of Pt^{IV} ions through electronic interactions. The low activity of Co^{II}[Pt^{IV}(CN)₆] in O₂ evolution suggested that the presence of

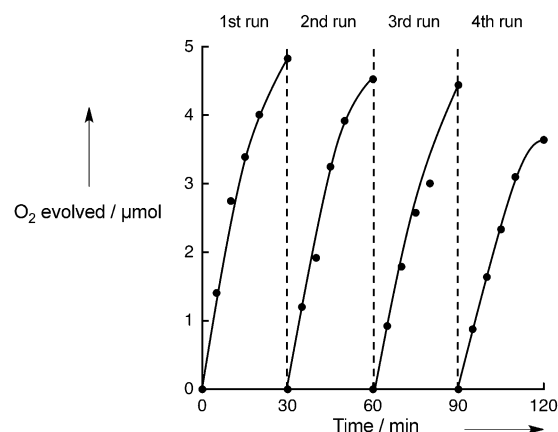


Figure 4. Time courses of O₂ evolution by visible-light irradiation ($\lambda > 420$ nm) of a phosphate buffer (2.0 mL, 50 mM, pH 8.0) containing [Ru(bpy)₃]²⁺ (1.0 mM), Na₂S₂O₈ (5.0 mM), and [Co(H₂O)_{1.79}]_{1.42}[(Co^{III}_{0.85}Pt^{IV}_{0.15})(CN)₆] (800 μg). A small portion of a concentrated Na₂S₂O₈ solution was added to the reaction solution to make a concentration of Na₂S₂O₈ 5.0 mM after O₂ evolution ceased.

labile coordination sites on the Co^{II} ion is as crucial to the oxidation ability.

The robustness of [Co^{II}(H₂O)_{1.79}]_{1.42}[(Co^{III}_{0.85}Pt^{IV}_{0.15})(CN)₆] was confirmed by the repetitive addition of an aliquot (100 μL) of Na₂S₂O₈ to the reaction solution after cessation of O₂ evolution. O₂ yields higher than 90% were attained for up to three runs (Figure 4). The spent catalyst was collected by centrifugation and used for IR spectrum and powder X-ray diffraction measurements. The IR spectrum measurements of the spent sample showed no changes in peak positions and relative intensities of the two ν(CN) peaks at 2236 and 2175 cm⁻¹ compared to those of the fresh sample (see Figure S4). [Co^{II}(H₂O)₂]_{1.5}[Co^{III}(CN)₆] has been reported to lose catalytic activity for water oxidation by binding bipyridine, as evidenced by IR and Raman spectroscopy.^[10b] Adsorption of [Ru(bpy)₃]²⁺ or bpy onto the [Co^{II}(H₂O)_{1.79}]_{1.42}[(Co^{III}_{0.85}Pt^{IV}_{0.15})(CN)₆] after photocatalytic O₂ evolution was also confirmed by the IR spectroscopy, however, the deceleration effect of the adsorbent was limited. The XRD peaks of the spent sample also contained all the same peaks as those observed for the fresh sample (see Figure S5). These results assure the robustness of the [Co^{II}(H₂O)_{1.79}]_{1.42}[(Co^{III}_{0.85}Pt^{IV}_{0.15})(CN)₆].

The effects of structural modifications of the framework were confirmed by investigating the catalysis of [Co^{II}(H₂O)₂]_n[(Co^{III}(CN)₆]_{1-x}[Pt^{II}(CN)₄]_x] ($n' = 1.5-0.5x$), which contains Pt^{II} ions with a square-planar coordination structure instead of Pt^{IV} ions with an octahedral structure. The Co^{II} ions in the complexes possess two H₂O molecules as external ligands, independent of content of Pt^{II} ions (see note on page S3). When no Co^{III} ion was included in a complex, the powder X-ray diffraction pattern indicated that the complex has a planar structure, not a cubic structure. However, complexes containing both Co^{III} and Pt^{II} ions provided diffraction patterns indicating a cubic structure which is isostructural to Prussian blue (Figure 5a). Also, and N₂ the adsorption-desorption isotherm indicated the presence of micropores with high BET surface areas (see Figure S2b). A schematic

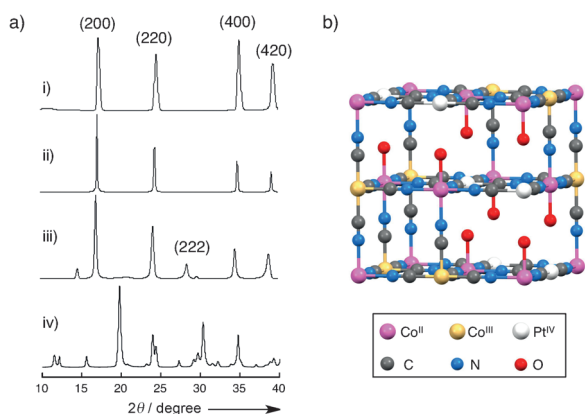


Figure 5. a) Powder X-ray diffraction patterns of a series of heteropolynuclear cyanide complexes, $[\text{Co}^{\text{II}}(\text{H}_2\text{O})_2]_n[\{\text{Co}^{\text{III}}(\text{CN})_6\}_{1-x}\{\text{Pt}^{\text{II}}(\text{CN})_4\}_x]$. i) $x=0$, ii) $x=0.37$, iii) $x=0.60$, and iv) $x=1$. b) A schematic drawing of $[\text{Co}^{\text{II}}(\text{H}_2\text{O})_2]_n[\{\text{Co}^{\text{III}}(\text{CN})_6\}_{1-x}\{\text{Pt}^{\text{II}}(\text{CN})_4\}_x]$. Hydrogen atoms of water molecules are omitted.

drawing of a typical structure of $[\text{Co}^{\text{II}}(\text{H}_2\text{O})_2]_n[\{\text{Co}^{\text{III}}(\text{CN})_6\}_{1-x}\{\text{Pt}^{\text{II}}(\text{CN})_4\}_x]$ is depicted in Figure 5b.

Photocatalytic water oxidation was performed by photoirradiation ($\lambda > 420 \text{ nm}$) of a phosphate buffer (2.0 mL, 50 mM, pH 8.0) containing $[\text{Ru}(\text{bpy})_3]^{2+}$ (1.0 mM), $\text{Na}_2\text{S}_2\text{O}_8$ (5.0 mM), and $[\text{Co}^{\text{II}}(\text{H}_2\text{O})_2]_n[\{\text{Co}^{\text{III}}(\text{CN})_6\}_{1-x}\{\text{Pt}^{\text{II}}(\text{CN})_4\}_x]$ (80 μg) with various amounts of Pt^{II} ions (Figure 6). The

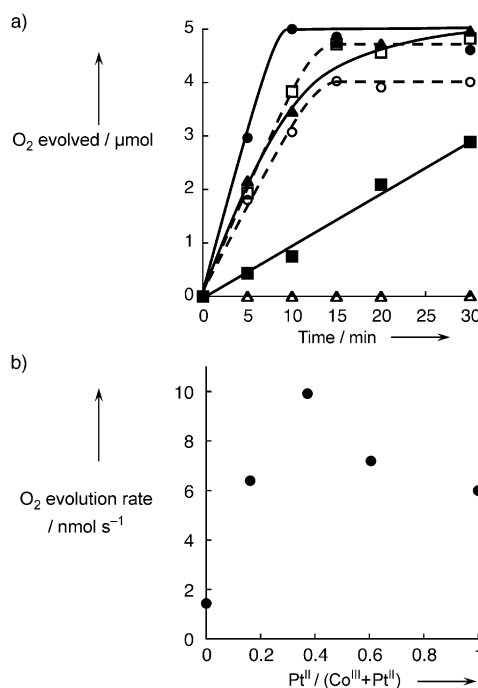


Figure 6. a) Time courses of O_2 evolution by visible-light irradiation ($\lambda > 420 \text{ nm}$) of a phosphate buffer (2.0 mL, 50 mM, pH 8.0) containing $[\text{Ru}(\text{bpy})_3]^{2+}$ (1.0 mM), $\text{Na}_2\text{S}_2\text{O}_8$ (5.0 mM), and a heteropolynuclear cyanide complex, $[\text{Co}^{\text{II}}(\text{H}_2\text{O})_2]_n[\{\text{Co}^{\text{III}}(\text{CN})_6\}_{1-x}\{\text{Pt}^{\text{II}}(\text{CN})_4\}_x]$ (80 μg). $x=0$ (closed square); $x=0.16$ (open square); $x=0.37$ (closed circle); $x=0.60$ (closed triangle) and $x=1$ (open circle). Time course of O_2 evolution under dark conditions using the complex with $x=0.37$ (open triangle) b) Initial O_2 evolution rates ($< 5 \text{ min}$) at different Pt^{II} ion contents in $[\text{Co}^{\text{II}}(\text{H}_2\text{O})_2]_n[\{\text{Co}^{\text{III}}(\text{CN})_6\}_{1-x}\{\text{Pt}^{\text{II}}(\text{CN})_4\}_x]$.

initial O_2 evolution rate (5 min) of $[\text{Co}^{\text{II}}(\text{H}_2\text{O})_2][\text{Pt}^{\text{II}}(\text{CN})_4]$ (6.0 nmol s^{-1}) was much higher than that of $\text{Co}^{\text{II}}[\text{Pt}^{\text{IV}}(\text{CN})_6]$ (0.50 nmol s^{-1}), and results from the presence of water molecules coordinating the Co^{II} ions. The initial O_2 evolution rates increased by decreasing the Pt^{II} ion content to 0.37, wherein the initial O_2 evolution rate exceeded 9.9 nmol s^{-1} , with a nearly stoichiometric amount of O_2 evolution. An apparent quantum yield of 50% was determined by using monochromatic light with a $\lambda = 450 \text{ nm}$ wavelength (see Figure S6). The high O_2 -evolution rates, in accord with a decrease in the Pt^{II} ion content, resulted from a larger number of Co^{II} ions serving as active sites. The low O_2 evolution rates at low Pt^{II} ion content (0.16 and 0) may result from the decrease in the available space inside the crystals thus resulting from an increase in the number of coordinatively saturated $[\text{Co}^{\text{III}}(\text{CN})_6]^{3-}$.

Repetitive experiments using $[\text{Co}^{\text{II}}(\text{H}_2\text{O})_2]_{1.31}[\{\text{Co}^{\text{III}}(\text{CN})_6\}_{0.63}\{\text{Pt}^{\text{II}}(\text{CN})_4\}_{0.37}]$ (800 μg) as a WOC were performed by the same procedure as that used for the experiments with $[\text{Co}^{\text{II}}(\text{H}_2\text{O})_{1.79}]_{1.42}[\{\text{Co}^{\text{III}}_{0.85}\text{Pt}^{\text{IV}}_{0.15}\}(\text{CN})_6]$. O_2 yields higher than 80% were obtained for three runs (see Figure S7). The XRD pattern and $\nu(\text{CN})$ in the IR spectra of $[\text{Co}^{\text{II}}(\text{H}_2\text{O})_2]_{1.31}[\{\text{Co}^{\text{III}}(\text{CN})_6\}_{0.63}\{\text{Pt}^{\text{II}}(\text{CN})_4\}_{0.37}]$, after the reaction, were the same as those of the fresh catalyst (see Figures S8). IR spectra indicated the strong adsorption of the negatively charged SO_4^{2-} on $[\text{Co}^{\text{II}}(\text{H}_2\text{O})_2]_{1.31}[\{\text{Co}^{\text{III}}(\text{CN})_6\}_{0.63}\{\text{Pt}^{\text{II}}(\text{CN})_4\}_{0.37}]$, however, no adsorption of the positively charged $[\text{Ru}(\text{bpy})_3]^{2+}$ or neutral bpy, which adsorbed on $[\text{Co}^{\text{II}}(\text{H}_2\text{O})_{1.79}]_{1.42}[\{\text{Co}^{\text{III}}_{0.85}\text{Pt}^{\text{IV}}_{0.15}\}(\text{CN})_6]$, was confirmed. These results may reflect the nature of defect sites of each complex.

In conclusion, a near-stoichiometric amount of O_2 evolution was observed in visible-light ($\lambda > 420 \text{ nm}$) driven water oxidation, which was efficiently catalyzed by heteropolynuclear cyanide complexes containing both cobalt and platinum ions. The addition of $\text{Pt}^{\text{IV}}(\text{CN})_6^{2-}$ units to cobalt cyanide complexes enhanced the catalysis for water oxidation by increasing the oxidation potential of N-bound Co^{II} ions acting as active sites. When $\text{Pt}^{\text{II}}(\text{CN})_4^{2-}$ units were introduced to cobalt cyanide complexes, the hollow structure enabled utilization of space inside the crystals. These results suggest that platinum ions, irrespective of the valence, are effective in enhancing the catalytic activity of cobalt cyanide complexes through electronic and structural modifications. The strategy to utilize heteropolynuclear cyanide complexes reported in this study provides a convenient way to develop efficient water-oxidation catalysts.

Experimental Section

Heteropolynuclear cyanide complexes were prepared by mixing an aqueous solution containing $\text{K}_3[\text{Co}^{\text{III}}(\text{CN})_6]$ and either $\text{K}_2[\text{Pt}^{\text{IV}}(\text{CN})_6]$ or $\text{K}_2[\text{Pt}^{\text{II}}(\text{CN})_4]$ with an aqueous solution containing $\text{Co}(\text{NO}_3)_2$ to form precipitates. The Co^{III} and Pt^{IV} ion contents in a prepared complex were determined by X-ray fluorescence measurements (Rigaku ZSX 1000/MPS). A typical procedure for a catalysis measurement is as follows: a heteropolynuclear cyanide complex (80 μg) was suspended to a phosphate buffer (pH 8.0, 50 mM, 2.0 mL) containing $[\text{Ru}(2,2'\text{-bipyridine})_3]\text{SO}_4$ (1.0 mM) and $\text{Na}_2\text{S}_2\text{O}_8$ (5.0 mM) under Ar atmosphere. After photoirradiation ($\lambda > 420 \text{ nm}$) of the

suspension with magnetic stirring, an aliquot of headspace gas was analyzed to determine the amount of evolved O₂ by a gas chromatograph (Shimadzu GC-17A equipped with a molecular sieve 5A column and thermal conductivity detector). Repetitive reactions were conducted by addition of Na₂S₂O₈ to a reaction solution after cessation of O₂ evolution where the pH of the solution was adjusted to a certain value. The experimental details about chemicals and other characterization of complexes are described in the Supporting Information.

Keywords: cobalt · heterogeneous catalysis · platinum · structure elucidation · water oxidation

How to cite: *Angew. Chem. Int. Ed.* **2015**, *54*, 5613–5617
Angew. Chem. **2015**, *127*, 5705–5709

- [1] a) H. B. Gray, *Nat. Chem.* **2009**, *1*, 7–7; b) D. G. Nocera, *Acc. Chem. Res.* **2012**, *45*, 767–776.
- [2] a) J. M. Thomas, *Energy Environ. Sci.* **2014**, *7*, 19–20; b) J. A. Herron, J. Kim, A. A. Upadhye, G. W. Huber, C. T. Maravelias, *Energy Environ. Sci.* **2015**, *8*, 126–157; c) J. R. McKone, N. S. Lewis, H. B. Gray, *Chem. Mater.* **2014**, *26*, 407–414.
- [3] a) J. J. Concepcion, R. L. House, J. M. Papanikolas, T. J. Meyer, *Proc. Natl. Acad. Sci. USA* **2012**, *109*, 15560–15564; b) S. Fukuzumi, Y. Yamada, *ChemSusChem* **2013**, *6*, 1834–1847; c) S. Berardi, S. Drouet, L. Francas, C. Gimbert-Surinach, M. Guttentag, C. Richmond, T. Stoll, A. Llobet, *Chem. Soc. Rev.* **2014**, *43*, 7501–7519.
- [4] a) A. Sartorel, M. Carraro, F. M. Toma, M. Prato, M. Bonchio, *Energy Environ. Sci.* **2012**, *5*, 5592–5603; b) S. Fukuzumi, D. Hong, Y. Yamada, *J. Phys. Chem. Lett.* **2013**, *4*, 3458–3467; c) K. J. Young, L. A. Martini, R. L. Milot, R. C. Iii, V. S. Batista, C. A. Schmuttenmaer, R. H. Crabtree, G. W. Brudvig, *Coord. Chem. Rev.* **2012**, *256*, 2503–2520.
- [5] a) D. G. H. Hettterscheid, L. Sun, *Eur. J. Inorg. Chem.* **2014**, 571–572; b) M. D. Kärkäs, E. V. Johnston, O. Verho, B. Åkermark, *Acc. Chem. Res.* **2014**, *47*, 100–111; c) M. D. Kärkäs, O. Verho, E. V. Johnston, B. Åkermark, *Chem. Rev.* **2014**, *114*, 11863–12001; d) A. R. Parent, K. Sakai, *ChemSusChem* **2014**, *7*, 2070–2080.
- [6] a) A. Harriman, I. J. Pickering, J. M. Thomas, P. A. Christensen, *J. Chem. Soc. Faraday Trans. 1* **1988**, *84*, 2795–2806; b) F. Jiao, H. Frei, *Energy Environ. Sci.* **2010**, *3*, 1018–1027.
- [7] a) J. L. Boyer, J. Rochford, M.-K. Tsai, J. T. Muckerman, E. Fujita, *Coord. Chem. Rev.* **2010**, *254*, 309–330; b) J. R. Galán-Mascarós, *ChemElectroChem* **2015**, *2*, 37–50; c) M. Hirahara, A. Shoji, M. Yagi, *Eur. J. Inorg. Chem.* **2014**, 595–606; d) X. Sala, S. Maji, R. Bofill, J. Garcia-Anton, L. Escriche, A. Llobet, *Acc. Chem. Res.* **2014**, *47*, 504–516; e) A. Singh, L. Spiccia, *Coord. Chem. Rev.* **2013**, *257*, 2607–2622; f) D. J. Wasylenko, R. D. Palmer, C. P. Berlinguette, *Chem. Commun.* **2013**, 49, 218–227.
- [8] a) J. J. Stracke, R. G. Finke, *ACS Catal.* **2014**, *4*, 909–933; b) J. D. Blakemore, N. D. Schley, G. W. Olack, C. D. Incarvito, G. W. Brudvig, R. H. Crabtree, *Chem. Sci.* **2011**, *2*, 94–98; c) D. Hong, M. Murakami, Y. Yamada, S. Fukuzumi, *Energy Environ. Sci.* **2012**, *5*, 5708–5716; d) D. Hong, J. Jung, J. Park, Y. Yamada, T. Suenobu, Y.-M. Lee, W. Nam, S. Fukuzumi, *Energy Environ. Sci.* **2012**, *5*, 7606–7616.
- [9] a) M. Zhang, H. Frei, *Catal. Lett.* **2015**, *145*, 420–435; b) D. Hong, Y. Yamada, T. Nagatomi, Y. Takai, S. Fukuzumi, *J. Am. Chem. Soc.* **2012**, *134*, 19572–19575; c) Y. Yamada, K. Yano, D. Hong, S. Fukuzumi, *Phys. Chem. Chem. Phys.* **2012**, *14*, 5753–5760.
- [10] a) T. Zhang, W. Lin, *Chem. Soc. Rev.* **2014**, *43*, 5982–5993; b) S. Goberna-Ferrón, W. Y. Hernández, B. Rodríguez-García, J. R. Galán-Mascarós, *ACS Catal.* **2014**, *4*, 1637–1641; c) S. Pintado, S. Goberna-Ferron, E. C. Escudero-Adan, J. R. Galan-Mascaros, *J. Am. Chem. Soc.* **2013**, *135*, 13270–13273.
- [11] a) H. J. Buser, D. Schwarzenbach, W. Petter, A. Ludi, *Inorg. Chem.* **1977**, *16*, 2704–2710; b) X.-P. Shen, Y.-Z. Li, Y. Song, Z. Xu, G.-C. Guo, *Eur. J. Inorg. Chem.* **2007**, 1698–1702.
- [12] Y. Yamada, M. Yoneda, S. Fukuzumi, *Chem. Eur. J.* **2013**, *19*, 11733–11741.
- [13] a) J. M. Herrera, A. Bachschmidt, F. Villain, A. Bleuzen, V. Marvaud, W. Wernsdorfer, M. Verdaguer, *Philos. Trans. R. Soc. London Ser. A* **2008**, *366*, 127–138; b) M. Verdaguer, G. S. Girolami in *Magnetism: molecules to materials*, Vol. V (Eds.: J. S. Miller, M. Drillon), Wiley-VCH, Weinheim, **2005**.
- [14] R. D. Shannon, *Acta Crystallogr. Sect. A* **1969**, *32*, 751–767.
- [15] M. R. Robin, *Inorg. Chem.* **1962**, *1*, 337–342.
- [16] M. Hara, C. C. Waraksa, J. T. Lean, B. A. Lewis, T. E. Mallouk, *J. Phys. Chem. A* **2000**, *104*, 5275–5280.

Received: February 5, 2015

Revised: March 9, 2015

Published online: April 13, 2015